Analysis of the Effectiveness of Ground-based VLF Wave Observations for Predicting or Nowcasting Relativistic Electron Flux at Geostationary Orbit

Laura E. Simms, Augsburg College, Minneapolis, MN, USA

(*simmsl@augsburg.edu*)

Mark J. Engebretson, Augsburg College, Minneapolis, MN, USA

A.J. Smith, VLF ELF Radio Research Institute, Bradwell, UK

Mark Clilverd, British Antarctic Survey, Cambridge, UK

Viacheslav Pilipenko, Institute of the Physics of the Earth, Moscow, Russia

Geoffrey D. Reeves, Los Alamos National Laboratory, NM, USA

This article has been accepted for publication and undergone full peer review but has not been through the copyediting, typesetting, pagination and proofreading process which may lead to differences between this version and the Version of Record. Please cite this article as doi: 10.1002/2014JA020337

Abstract

Post-storm relativistic electron flux enhancement at geosynchronous orbit has shown correlation with very low frequency (VLF) waves measured by satellite in situ. However, our previous study found little correlation between electron flux and VLF measured by a ground-based instrument at Halley, Antarctica. Here we explore several possible explanations for this low correlation. Using 220 storms (1992-2002), our previous work developed a predictive model of the post-storm flux at geosynchronous orbit based on explanatory variables measured a day or two before the flux increase. In a nowcast model, we use averages of variables from the time period when flux is rising during the recovery phase of geomagnetic storms, and limit the VLF (1.0 kHz) measure to the dawn period at Halley (9-12 UT). This improves the simple correlation of VLF wave intensity with flux, although the VLF effect in an overall multiple regression is still much less than that of other factors. When analyses are performed separately for season and IMF Bz orientation, VLF outweighs the influence of other factors only during winter months when IMF Bz is in an average northward orientation.

Key Points:

- Dawn ground VLF waves correlate with relativistic flux
- Best ground VLF-flux correlations in winter during northward IMF Bz conditions
- In multiple regression, VLF-flux correlation low compared to other factors

Index Terms:

Radiation belts

Magnetic storms and substorms

Forecasting

Wave/particle interactions

Keywords:

Relativistic electron flux

VLF waves

1. Introduction

A number of studies have found an association between relativistic electron enhancement and very low frequency (VLF) magnetospheric waves measured on the ground [Meredith et al., 2003; Smith et al., 2004] and by satellite [O'Brien et al., 2003; Miyoshi et al., 2013]. As well, there are many examples of satellite observations of VLF waves leading directly to relativistic electron flux enhancement [Horne et al., 2005; Thorne et al., 2013; Li et al., 2014; Su et al., 2014; Turner et al., 2014; Xiao et al., 2014]. Successful models of the acceleration of seed electrons to relativistic energies by VLF waves alone have also been produced [e.g., Albert et al., 2009; Tu et al., 2014], as well as physics-based models incorporating wave-particle interactions as one of many key processes [Horne et al., 2013].

Numerous studies have shown correlations between relativistic electron flux levels and parameters such as solar wind velocity and number density [Blake et al., 1997; Baker et al., 1998b; O'Brien et al., 2001; Reeves et al., 2003; Weigel et al., 2003; Ukhorskiy et al., 2004; Lyons et al., 2005; Lyatsky and Khazanov, 2008a and 2008b; Balikhin et al., 2011; Reeves et al., 2011; Kellerman and Shprits, 2012; Potapov et al., 2012; Potapov et al., 2014], Dst, Kp, and AE indices [Baker et al., 1990; Dimitriev and Chao, 2003; Meredith et al., 2003; Li et al., 2009; Lyatsky and Khazanov, 2008b; Ukhorskiy et al., 2004], interplanetary magnetic field Bz (IMF Bz) [Blake et al., 1997; Iles et al., 2002; Miyoshi and Kataoka, 2008; Miyoshi et al., 2013], and ULF (ultra low frequency) wave power [Rostoker et al., 1998; Mathie and Mann, 2000; O'Brien et al., 2003; Kozyreva et al., 2007; Romanova and Pilipenko, 2008; Borovsky and Denton, 2014; Potapov et al., 2014]. Although a correlation between a factor and relativistic flux does not prove that factor causes increased flux, a lack of positive correlation would suggest it is not involved in electron acceleration. However, no matter what the mechanism is, a strong correlation between a parameter and increasing relativistic flux means that factor can be used as a predictor of increased flux.

In a previous paper, we found that many solar wind and magnetosphere parameters, as well as a ULF wave index, could be used to predict relativistic electron flux levels at geostationary orbit following storms using a data-based model produced by multiple regression [Simms et al., 2014]. As many of these factors are correlated among themselves, we developed models that attempted to determine which of these factors correlated with and predicted flux best when all factors were present in the model. This extended the work of previous multi-factor, data-based models [Lyatsky and Khazanov, 2008b; Ukhorskiy et al., 2004; Balikhin et al., 2011; Kellerman and Shprits, 2012; Borovsky and Denton, 2014].

However, in our previous models [Simms et al., 2014], ground-based measurements of VLF magnetospheric waves (~1 kHz) showed little ability to predict enhanced relativistic electron flux 24 hours later. In the present study, we suggest several possible explanations for why ground-based VLF does not work well as a predictor.

Previously, we attempted to predict flux more than 72 hours after the minimum Dst of a storm using variables averaged over three time periods: pre-storm, main phase, and early recovery phase (48 hours immediately following the minimum Dst). ULF wave power, seed electron flux, solar wind velocity and its variation, and after-storm IMF Bz were the most significant explanatory variables in these regression models. However, any factor that operated at a short time scale on flux would be missed by this approach, as predictors were measured no less than 24 hours in advance of the flux measurement. A nowcast model would be more appropriate for studying short term actions.

Our previous paper used a daily average of VLF wave power from the Halley VELOX instrument, which does not discriminate between chorus and hiss in several bandpass spectral windows [Smith et al., 2010]. However, VLF waves may be responsible for both increases in flux due to acceleration of electrons by chorus waves and decreases due to precipitation caused by hiss [Kessel, 2012]. Therefore, averaging the entire 24 hr MLT period may result in a measure that cannot distinguish between the opposing effects of acceleration and precipitation. In our current study, we compare the 24 hr average with VLF averaged only over the dawn period (9-12 UT at Halley) when dawn chorus dominates (06-09 MLT) [Smith et al., 2010].

Seasonal effects may be a third explanation for why VLF waves showed so little influence in our previous predictive models. This may be due to two reasons. First, the ground VLF wave power measured at Halley that we use may vary between seasons. Solar illumination of the ionosphere in the southern hemisphere summer months (October-February) at Halley has been found to reduce the VLF wave amplitude in the 1-3 kHz range [Smith et al., 2010]. Thus, the apparent influence of VLF waves may be artificially lowered during these time periods when its measured amplitude is reduced.

Besides this measurement effect of season, the geoeffectiveness of solar wind parameters may vary by season as a result of IMF Bz orientation relative to the Earth's magnetosphere changing as the year progresses [Russell and McPherron, 1973; Mc Pherron et al., 2009]. Although our previous paper controlled for a Bz effect, we did not control for season, nor study how the Bz effect (or that of other parameters) might behave in different seasons.

The thrust of this current paper is therefore threefold: 1) to produce nowcast models as a complement to our predictor models to determine whether ground VLF power has more correlation with flux at more immediate timescales, 2) to study whether limiting the ground VLF measure to the dawn period results in more correlation with flux, and 3) to explore the effect of season on the ground VLF-flux correlation. The refinement of the model using these approaches may allow the use of ground VLF to predict relativistic electron flux.

To do this, we again use the technique of multiple regression. This allows the straightforward addition of predictor variables, as well as determining which predictors are most significant when all other factors are held constant [Neter et al., 1985; Simms et al., 2010; Golden et al., 2012].

2. Methods

As described more fully in Simms et al. (2014), we identified 220 storms (1992-2002) with at least 72 storm-free hours after the end of recovery (when Dst returns above -30 nT). We used the 1.0 kHz VELOX channel of Halley VLF (this channel includes frequencies from 0.5 to 1.5 kHz) as it showed the most influence in simple correlations and the multiple regressions. This channel corresponds to an L_{max} of 7.52 and will detect VLF from L-shells below 7.52, including those at geosynchronous orbit (L = 6.6) [Smith et al., 2004; Smith, 1995]. Our initial analyses used the 24 hr (MLT) average of VLF wave power. However, in later analyses we use the average of VLF wave power only from the dawn period at Halley (9-12 UT, 6-9 MLT). This time period was chosen as that in which dawn chorus would be the strongest influence [Smith et al., 2010]. Only 191 storms remained in this data set as not all had VLF observations in this time period.

We obtained hourly averaged electron fluxes for relativistic electrons (> 1.5 MeV) and seed electrons (75-105 keV) from several spacecraft (Los Alamos National Laboratory (LANL) geosynchronous energetic particle instruments at approximately 6.6 R_E). We calculated the maximum relativistic electron flux of these hourly averages in the 48-120 hours following each storm.

As additional predictor variables we used a ground-based ULF index [Kozyreva et al., 2007] (2-7 mHz, covering local times 0500 – 1500, characterizing the maximal hourly value of ULF wave power over the entire globe). All wave power variables were $\log_{10}$ values. In addition, we obtained IMF Bz (GSM coordinates) and solar wind velocity (Vx in GSM coordinates. In preliminary analyses, we discovered that the correlation between Vx and number density was too high to allow the use of both in our multiple regression models. As number density entered the models as a negative factor, we chose to use Vx.

All variables were converted to rankit normal scores (Sokal and Rohlf, 1995) by assigning a rank to each observation and then replacing that rank with the value of the same ranked order statistic from a normal distribution. This transformation converted the data into a normal distribution and allowed the use of linear regression, even if the original variables were related in a non-linear way. Statistical analyses were performed in SPSS (Statistical Package for the Social Sciences) and IDL (Interactive Data Language).

We found the average of each solar wind and IMF predictive variable during two storm periods: early recovery phase (0-48 hours after the minimum Dst), and late recovery (48-72 hours after minimum Dst). Regressions using the first time period were used to predict flux 48-120 hours after the minimum Dst. Regressions using the second time period were used to nowcast flux. Although we included up to 120 hrs after minimum Dst in which to find the maximum flux, most of the rise in flux occurs by 72 hrs and the levels remain fairly constant in the latter half of this time period [Borovsky and Denton, 2009]. Other variables, however, drop off during this time period, so an average of them over this entire time period would give artificially low values.

Full regression models are given for the full dataset (all seasons combined), but when the dataset is split into seasons the sample sizes become too low to keep all variables in the models. The seasonal models were therefore reduced using backward elimination. This is a type of stepwise regression used to choose the most explanatory variables. This method adds all variables to the model at the beginning, then drops those which show no significant effect

[Hocking 1976]. After each variable is removed, a regression is run again with the reduced set, and the next variable that does not meet the criterion for inclusion dropped. The algorithm stops when all remaining predictor variables meet the significance criterion. We set the level at which to remove a variable at a p-value > 0.10. The p-value is the estimated probability of mistakenly rejecting a null hypothesis when that hypothesis is actually true. Statistical significance is often set at $p < 0.05$, so the 0.10 criterion will conservatively include more variables in a model rather than discarding them. This method is a means of producing a model that is not over-fitted, while retaining all variables that may show an influence. (Other regression techniques such as ridge regression, principal components regression, or partial least squares regression (discussed in Hastie et al., 2009) might be used with data sets such as this to reduce multicollinearity, but these methods either make statistical tests impossible or obscure the relative influence of predictors. For these reasons, we have continued to use ordinary least squares regression.)

In a previous study, validation of similar models (based on the same dataset) was performed with a training set of a semi-random sample of 4/5 of the storms (spread over all years and seasons) and the remaining 1/5 as the validation set (with a similar spread over years and seasons) [Simms et al., 2014].

Only 191 storms remained in the dataset when VLF was averaged only over the dawn period (9-12 UT). Within this set, there were 44 storms in the Dec-Feb period, 60 in Mar-May, 41 in Jun-Aug, and 46 in Sep-Nov.

When models were split by IMF Bz orientation, the northward Bz category included all those storms where the Bz averaged over the time period in question was positive (0-48 hours after minimum Dst for the prediction models, 48-72 hours for the nowcast models). The southward category included those where the Bz average was negative.

3. Results

Halley ground VLF wave amplitude following storms is significantly lower during the height of southern hemisphere summer (Dec-Feb) (Figure 1). This is true of VLF waves measured in early recovery (0-48 hours after minimum Dst -- the "predictor" variable set) and in late recovery (48-72 hours after minimum Dst -- the "nowcast" variable set). It is also seen in both VLF averaged over the entire 24 hour period and that averaged only during the dawn (9-12 UT) when the dawn chorus is strongest.

Of all the predictor variables, VLF averaged over the full 24 hour MLT period showed the least correlation with relativistic electron flux in both the prediction and the nowcast models (Figure 2). When averaged only over 9-12 UT (dawn), VLF was somewhat more correlated with flux. We use this subset of dawn-averaged VLF power in all the remaining analyses.

Of the four VELOX frequency channels studied (0.5, 1.0, 2.0, and 4.25 kHz), the highest correlation of dawn VLF wave power (9-12 UT) with relativistic electron flux occurs with the nowcast 1.0 kHz channel (Table 1). The slightly lower correlations seen with VLF 24 hours previous may suggest that VLF acts at a more immediate time scale. All other variables show modestly more correlation as predictors than as nowcasters (Figure 2).

When VLF-flux correlations are broken down by both season and IMF Bz orientation, VLF shows the highest correlation during periods of northward Bz (Figure 3). This is most pronounced in the winter months (Jun-Aug).

The full multiple regressions over all seasons show few differences between the prediction and nowcast models. Main phase seed electron flux, ULF power, Vx, and IMF Bz are significant correlates when measured in the early recovery (0-48 hours following minimum Dst; prediction – Figure 4A) and when measured in the late recovery (48-72 hours following minimum Dst; nowcast – Figure 4B). VLF power is not a significant influence in either the prediction or the nowcast model when all seasons are combined.

As nowcast and prediction models were similar, and as nowcast simple correlations were slightly higher, only the nowcast data is used in the seasonal break down analyses. When seasons are analyzed separately, the sample sizes became too low to keep all variables in the models. Therefore, reduced models were produced by backward-elimination stepwise regression, in which most non-significant variables ($p > 0.10$) were dropped. Figure 5 shows nowcast models by season (explanatory variables averaged over late recovery -- 48-72 hours after minimum Dst). VLF wave power is retained only in the Jun-Aug period, although it is not statistically significant.

As the VLF influence appears to vary by both season and IMF Bz orientation, we analyzed subsets broken down by both these factors (Figure 6). We show only those regression models in which VLF showed a significant influence (Mar-May and Jun-Aug, the winter months in the southern hemisphere). VLF was the only significant factor during periods of northward Bz in these winter months, but it was not a factor during periods of southward Bz in winter months.

4. Discussion

As in our previous study [Simms et al., 2014], other variables (seed electron flux, ULF wave index, Vx, and IMF Bz) show more ability to predict relativistic electron flux than VLF waves, whether in simple correlation analysis or in multiple regression models. However, VLF wave power was found to be a correlate with relativistic electron flux in other studies of both ground and satellite VLF [Meredith et al., 2003; O'Brien et al., 2003; Smith et al., 2004; Lyons et al., 2005; Miyoshi et al., 2013; Thorne et al., 2013]. We hypothesize several reasons why we may be finding different results.

Within the broad class of VLF waves, chorus waves are thought to accelerate electrons while hiss is believed to cause electron precipitation [Kessel, 2012]. Both dawn chorus and afternoon hiss are picked up by the Halley VELOX instruments [Smith et al., 2010]. Averaging the two together may result in a measure that cannot distinguish between the opposing effects of acceleration and precipitation. Halley VELOX (at L-shell 4.5) is located such that it is close to the quiet time plasmapause field line footprint. Thus at ~1 kHz it will see a combination of VLF chorus waves (occurring outside the plasmapause) and plasmaspheric hiss (occurring inside the plasmapause), depending on the local time. This could reduce the correlation with post-storm relativistic fluxes, as plasmaspheric hiss takes no part in the electron acceleration process and may even be responsible for electron loss. By limiting our observations to the 9-12 UT period (dawn at Halley), we hoped to boost the contribution of dawn chorus which is hypothesized to cause electron acceleration. Limiting observations to the dawn period did improve the simple correlation we found between VLF wave power and relativistic flux enhancements, thus confirming the VLF correlation found in other studies that followed VLF waves [Meredith et al., 2003; O'Brien et al., 2003; Smith et al., 2004; Lyons et al., 2005; Miyoshi et al., 2013]. However, the magnitude of the correlation between flux and VLF wave power is still lower than that of most of the other tested variables.

Second, VLF waves may act more immediately. In our previous paper, we used average parameter values from the first 48 hours following minimum Dst to predict the rise in flux more than 48 hours after the minimum. However, a parameter that acted to increase flux within minutes or hours might have been missed with this approach. In our current study, we explore this possibility by comparing correlations and regression models between a prediction model (independent variables averaged over the first 48 hours) vs. a nowcast model (independent variables averaged over late recovery, 48-72 hours after minimum Dst). However, the nowcast correlation of 1.0 kHz VLF power is only slightly higher (Table 1). While this may account for some of the low correlation, it is not a major factor.

Although the simple correlation of VLF wave power with relativistic electron flux can be increased by restricting the VLF measurement to the dawn period (9-12 UT) and, to a lesser extent, by using a nowcast model, VLF still loses all significant influence in multiple regressions when other predictors are included in the model. This may be due to several other processes.

First, ground-measured VLF power may only be a significant explanatory factor in certain seasons. Ground VLF amplitude is reduced during summer months due to solar illumination of the ionosphere. Previously, this effect was found to reduce VLF amplitude in the 1-3 kHz range in the southern hemisphere summer months (October-February) at Halley, Antarctica [Smith et al., 2010]. We also found lower VLF amplitude in the Dec-Feb (summer) period as compared to other quarters of the year (Figure 1). As might be expected, our highest correlations with flux were in the winter months (Mar-May and Jun-Aug), but only when average recovery IMF Bz was in the northward direction.

The effectiveness of VLF waves only when IMF Bz is oriented northward would seem to contradict what is found in other studies. Miyoshi and Kataoka [2013] found that relativistic electron enhancements were more likely during southward Bz orientation, during which time VLF whistler waves also showed greater power. They concluded from this that the VLF acceleration of electrons was not effective during northward Bz, when both flux and VLF power were low. However, our correlation and regression analyses do not support this hypothesis. The only regression models in which VLF was found to be a significant factor were those from the winter months (Mar-May and, to a lesser extent, Jun-Aug) when only storms with average northward Bz were considered. Possibly, the reduction in other factors may mean they are less effective, allowing the VLF effect to be seen, or it may be that during periods of northward Bz, the Halley VELOX instrument is getting a truer picture of VLF power at geosynchronous orbit where the acceleration is taking place.

The field of view of the Halley VELOX receiver will be strongly influenced by the levels of subionospheric attenuation associated with propagation of the waves from more distant field lines, such as those of geosynchronous orbit at L = 6.6. The subionospheric distance of at least ~700 km from the L = 6.6 field line ionospheric exit point to the Halley receiver is equivalent to ~20dB attenuation at 1 kHz during the daytime (or summer) compared with ~10dB during the winter [Challinor, 1967]. Thus the receiver field of view is significantly wider during the winter months (Jun-Aug) than at other times. The slightly higher correlation between VLF waves and relativistic electron flux during Jun-Aug occurs when the VELOX field of view is able to pick up VLF wave power from the widest range of L shells.

Additionally, ground VLF observations are thought to be exclusively ducted waves, while satellite observations are rarely, if ever, made inside ducts [Walker 1971; Burgess and Inan, 2012]. The relationship between the two depends strongly on the efficiency of wave coupling into and out of ducts, which is probably quite variable [Rodger et al., 2010]. Electron acceleration can involve both ducted and nonducted chorus, but at a given moment in time, satellite observations in the non-ducted region may rarely correlate with ground observations along the ducts. Thus, it is not surprising that the Halley ground-based VLF wave power shows only a modest correlation (0.315 at best) with relativistic electron flux while satellite VLF observations show more association.

5. Conclusion

Our previous paper [Simms et al., 2014] found little correlation between ground VLF wave power and relativistic flux enhancement, although several previous studies had shown such a correlation. We have explored several possible explanations. We hypothesized that the VLF effect may be more immediate than that of the other explanatory variables, occurring within minutes or hours of the flux enhancement. However, a nowcast correlation of the VLF-flux correlation is only slightly higher when VLF waves are measured in late recovery (48-72 hours after the minimum Dst) than when they are measured immediately after the minimum Dst. Thus the VLF waves do not appear to act more immediately than other factors.

Limiting the ground VLF observations to 9-12 UT, the dawn period at Halley when chorus is at a maximum, had more impact on the correlation between VLF and relativistic electron flux. However, a multiple regression model using this refined measure still resulted in VLF having little influence when other factors are present.

The simple correlation of ground VLF with flux is somewhat higher during winter months (Jun-Aug in the southern hemisphere), and much higher when only storms with average northward IMF Bz during recovery are considered. Multiple regressions during these time periods show ground VLF to be a major correlate with relativistic electron flux, even when other factors are allowed in to the model.

However, ground VLF is not a useful parameter for predicting relativistic electron flux during most of the year. Satellite VLF measurements may be more strongly correlated with flux than ground-measured VLF. In future, we plan to compare the correlations of ground and satellite VLF waves with relativistic electron flux and to determine if satellite VLF measurements may be more useful in producing a predictive model.

Acknowledgements

Relativistic electron and seed electron flux data were obtained from Los Alamos National Laboratory (LANL) geosynchronous energetic particle instruments (PI: G. D. Reeves). Satellite and ground-based ULF indices may be obtained by contacting L. E. Simms, V. Pilipenko, or M. J. Engebretson. Halley VLF VELOX data is from M. Clilverd. IMF Bz, V, and Dst index are available from Goddard Space Flight Center Space Physics Data Facility at the OMNIWeb data website (http://omniweb.gsfc.nasa.gov/html/ow_data.html).

We thank the reviewers for their helpful comments.

This work was supported by National Science Foundation grants ATM-0827903 and AGS-1264146 to Augsburg College.

References

Albert, J. M., N. P. Meredith, and R. B. Horne (2009), Three-dimensional diffusion simulation of outer radiation belt electrons during the 9 October 1990 magnetic storm, J. Geophys. Res., 114(A09214) doi:10.1029/2009JA014336.

Baker, D. N., R. L. McPherron, T. E. Cayton, and R. W. Klebesadel (1990), Linear prediction filter analysis of relativistic electron properties at 6.6 RE, J. Geophys. Res., 95(A9), 133.

Baker, D.N., X Li, J.B Blake, S Kanekal (1998b), Strong electron acceleration in the

Earth's magnetosphere, Advances in Space Research, 21(4), 609-613.

Balikhin, M. A., R. J. Boynton, S. N. Walker, J. E. Borovsky, S. A. Billings, and H. L. Wei (2011), Using the NARMAX approach to model the evolution of energetic electrons fluxes at geostationary orbit, Geophys. Res. Lett., 38(L18105), doi:10.1029/2011GL048980.

Blake, J.B., D. N. Baker, N.Turner, K.W. Ogilvie, and R.P. Lepping (1997), Correlation of changes in the outer-zone relativistic-electron population with upstream solar wind and magnetic field measurements, Geophys. Res. Lett., 24(8), 927-929.

Borovsky, J. E. and M. H. Denton (2009), Relativistic-electron dropouts and recovery: A superposed epoch study of the magnetosphere and the solar wind, J. Geophys. Res., 114(A02201), doi:10.1029/2008JA013128.

Borovsky, J. E. and M. H. Denton (2014), Exploring the cross correlations and autocorrelations of the ULF indices and incorporating the ULF indices into the systems science of the solar wind-driven magnetosphere, J. Geophys. Res., 10.1002/2014JA019876.

Burgess, W. C., and U. S. Inan (1993), The role of ducted whistlers in the precipitation loss and equilibrium flux of radiation belt electrons, J. Geophys. Res., 98(A9), 15643–15665, doi:10.1029/93JA01202.

Challinor, R.A. (1967), The phase velocity and attenuation of audio-frequency electro-magnetic waves from simultaneous observations of atmospherics at two spaced stations, J. Atmos. and Terr. Phys., 29, 803–810, doi: 10.1016/0021-9169(67)90046-3.

Dmitriev, A.V. and J. K. Chao (2003), Dependence of geosynchronous relativistic electron enhancements on geomagnetic parameters, J. Geophys. Res., 108(A11), 1388, doi:10.1029/2002JA009664.

Golden, D. I., M. Spasojevic,W. Li, and Y. Nishimura (2012), Statistical modeling of plasmaspheric hiss amplitude using solar wind measurements and geomagnetic indices, GeophyS. Res. Lett., 39(L06103), doi:10.1029/2012GL051185.

Hastie, T., R. Tibshirani , J. Friedman (2009), The Elements of Statistical Learning: Data Mining, Inference, and Prediction, Second Edition (Springer Series in Statistics), Springer Publishing, New York, NY, 745 pages.

Hocking, R. R. (1976), The analysis and selection of variables in linear regression, Biometrics, 32, 1-49.

Horne, R. B., R. M. Thorne, S. A. Glauert, J. M. Albert, N. P. Meredith, and R. R. Anderson (2005), Timescale for radiation belt electron acceleration by whistler mode chorus waves, J. Geophys. Res., 110, A03225, doi:10.1029/2004JA010811.

Horne, R. B., S. A. Glauert, N. P. Meredith, D. Boscher, V. Maget, D. Heynderickx, and D. Pitchford (2013), Space weather impacts on satellites and forecasting the Earth's electron radiation belts with SPACECAST, Space Weather, 11, 1–18, doi:10.1002/swe.20023.

Iles, R. H. A., A. N. Fazakerley, A. D. Johnstone, N. P. Meredith, and P. Buhler (2002), The relativistic electron response in the outer radiation belt during magnetic storms, Ann. Geophys., 20, 957.

Kellerman, A.C. and Y. Y. Shprits (2012), On the influence of solar wind conditions on the outer-electron radiation belt, J. Geophys. Res., 117(A05217), doi:10.1029/2011JA017253.

Kessel, R. L. (2012), NASA's radiation belt storm probes mission: from concept to reality, 93-101, in Dynamics of the Earth's Radiation Belts and Inner Magnetosphere Geophys. Mongr. Ser. 199, ed: D. Summers, I. R. Mann, D. N. Baker, and M.G. Schulz.

Kozyreva, O. V., V. A. Pilipenko, M. J. Engebretson, and K. Yumoto (2007), A new ULF wave index and its comparison with dynamics of geostationary relativistic electrons, Planet. Space Sci., 55, 755–769.

Li, L. Y., J. B. Cao, G. C. Zhou, and X. Li (2009), Statistical roles of storms and substorms in changing the entire outer zone relativistic electron population, J. Geophys. Res., 114(A12214), doi:10.1029/2009JA014333.

Li, W., R. M. Thorne, Q. Ma, B. Ni, J. Bortnik, D. N. Baker, H. E. Spence, G. D. Reeves, S. G. Kanekal, J. C. Green, C. A. Kletzing, W. S. Kurth, G. B. Hospodarsky, J. B. Blake, J. F. Fennell and S. G. Claudepierre (2014), Radiation belt electron acceleration by chorus waves during the 17 March 2013 storm, J. Geophys. Res. Space Physics, 119, doi:10.1002/2014JA019945.

Lyatsky, W. and G. V. Khazanov (2008a), Effect of solar wind density on relativistic electrons at geosynchronous orbit, Geophys. Res. Lett., 35(L03109), doi:10.1029/2007GL032524.

Lyatsky, W and G. V. Khazanov (2008b), Effect of geomagnetic disturbances and solar wind density on relativistic electrons at geostationary orbit, J. Geophys. Res., 113(A08224), doi:10.1029/2008JA013048.

Lyons, L. R., D.-Y. Lee, R. M. Thorne, R. B. Horne, and A. J. Smith (2005), Solar wind-magnetosphere coupling leading to relativistic electron energization during high-speed streams, J. Geophys. Res., 110(A11202), doi:10.1029/2005JA011254.

Mathie, R.A. and I. R. Mann (2000), A correlation between extended intervals of ULF wave power and storm-time geosynchronous relativistic electron flux enhancements, Geophys. Res. Lett., 27(20), 3261-3264.

McPherron, R. L., D. N. Baker, and N. U. Crooker (2009), Role of the Russell-McPherron effect in the acceleration of relativistic electrons, J. Atmos. Sol.-Terr. Phys., 71, 1032–1044.

Meredith, N. P., M. Cain, R. B. Horne, R. M. Thorne, D. Summers, R. R. Anderson (2003), Evidence for chorus-driven electron acceleration to relativistic energies from a survey of geomagnetically disturbed periods, J. Geophys. Res., 108(A6), 1248, doi:10.1029/2002JA009764.

Miyoshi, Y. and R. Kataoka (2008), Flux enhancement of the outer radiation belt electrons after the arrival of stream interaction regions, J. Geophys. Res., 113(A03S09), doi:10.1029/2007JA012506.

Miyoshi, Y., R. Kataoka, Y. Kasahara, A. Kumamoto, T. Nagai, and M. F. Thomsen (2013), High-speed solar wind with southward interplanetary magnetic field causes relativistic electron flux enhancement of the outer radiation belt via enhanced condition of whistler waves, Geophys. Res. Lett., 40, doi:10.1002/grl.50916.

Neter, J., W. Wasserman, and M. H. Kutner (1985), Applied Linear Statistical Models, Richard D. Irwin, Inc., Homewood, IL, 1127 pages.

O'Brien, T.P., R . L. McPherron, and D. Sornette, G. D. Reeves, R. Friedel, and H. J. Singer (2001), Which magnetic storms produce relativistic electrons at geosynchronous orbit?, J. Geophys. Res., 106(A8), PAGES 15,533-15,54A4.

O'Brien, T. P., K. R. Lorentzen, I. R. Mann, N. P. Meredith, J. B. Blake, J. F. Fennell, M. D. Looper, D. K. Milling, and R. R. Anderson (2003), Energization of relativistic electrons in the presence of ULF power and MeV microbursts: Evidence for dual ULF and VLF acceleration, J. Geophys. Res., 108(A8), 1329, doi:10.1029/2002JA009784.

Potapov, A.S., B. Tsegmed, and L. V. Ryzhakova (2012), Relationship between the fluxes of relativistic electrons at geosynchronous orbit and the level of ULF activity on the earth’s surface and in the solar wind during the 23rd solar activity cycle, Cosmic Research, 50(2), pp. 124–140.

Potapov, A.S., B. Tsegmed, and L. V. Ryzhakova (2014), Solar cycle variation of “killer” electrons at geosynchronous orbit and electron flux correlation with the solar wind parameters and ULF waves intensity, Acta Astronautica, 93, 55-63.

Reeves, G. D. (1998), Relativistic electrons and magnetic storms: 1992-1995, Geophys. Res. Lett., 25(11), 1817-1820.

Reeves, G. D., K. L. McAdams, and R. H. W. Friedel (2003), Acceleration and loss of relativistic electrons during geomagnetic storms, Geophys. Res. Lett., 30(10), 1529, doi:10.1029/2002GL016513.

Reeves, G. D., S. K. Morley, R. H. W. Friedel, M. G. Henderson, T. E. Cayton, G. Cunningham, J. B. Blake, R. A. Christensen, and D. Thomsen (2011), On the relationship between relativistic electron flux and solar wind velocity: Paulikas and Blake revisited, J. Geophys. Res., 116(A02213), doi:10.1029/2010JA015735.

Rodger, C. J., B. R. Carson, S. A. Cummer, R. J. Gamble, M. A. Clilverd, J. C. Green, J.-A. Sauvaud, M. Parrot, and J.-J. Berthelier (2010), Contrasting the efficiency of radiation belt losses caused by ducted and nonducted whistler-mode waves from ground-based transmitters, J. Geophys. Res., 115(A12208), doi:10.1029/2010JA015880.

Romanova N., and Pilipenko V. (2008), ULF wave indices to characterize the solar wind – magnetosophere interaction and relativistic electron dynamics, Acta Geophysica, 57, N1, 158-170, doi:10.2478/s11600-008-0064-4.

Rostoker, G., S. Skone, and D. N. Baker (1998), On the origin of relativistic electrons in the magnetosphere associated with some geomagnetic storms, Geophys. Res. Lett., 25(19), 3701-3704.

Russell, C. T., and R. L. McPherron (1973), Semiannual variation of geomagnetic activity, J. Geophys. Res., 78, 92–108, doi:10.1029/JA078i001p00092.

Simms, L. E., V. A. Pilipenko, and M. J. Engebretson (2010), Determining the key drivers of magnetospheric Pc5 wave power, J. Geophys. Res., 115, A10241, doi:10.1029/2009JA015025.

Simms, L. E., V. A. Pilipenko, M. J. Engebretson G. D. Reeves, A.J. Smith, and M. Clilverd (2014), Prediction of relativistic electron flux at geostationary orbit following storms: Multiple regression analysis, J. Geophys. Res. Space Physics, 119, 10.1002/2014JA019955.

Smith, A. J. (1995), VELOX: A new VLF/ELF receiver in Antarctica for the Global Geospace Science mission, J. Atmos. Terr. Phys., 57(5), 507–524.

Smith, A. J., R. B. Horne, and N. P. Meredith (2010), The statistics of natural ELF/VLF waves derived from a long continuous set of ground-based observations at high latitude, J. Atmos. Terr. Phys., 72, 463-475.

Smith, A.J., Meredith N.P. and O'Brien T.P. (2004), Differences in ground-observed chorus in geomagnetic storms with and without enhanced relativistic electron fluxes, J. Geophys. Res., 109, A11204, doi:10.1029/2004JA010491.

Sokal, R.R., and F.J. Rohlf. 1995. Biometry: The principles and practice of statistics in biological research. 3rd edition. W.H. Freeman, New York, NY, 859p.

Su, Z., H. Zhu, F. Xiao, H. Zheng, Y. Wang, Z. He, C. Shen, C.Shen, C. B. Wang, R. Liu, M. Zhang, S. Wang, C. A. Kletzing, W. S. Kurth, G. B. Hospodarsky, H. E. Spence, G. D. Reeves, H. O. Funsten, J. B. Blake, D. N. Baker, and J. R.Wygant (2014), Intense duskside lower band chorus waves observed by Van Allen Probes: Generation and potential acceleration effect on radiation belt electrons, J. Geophys. Res. Space Physics, 119, 4266–4273, doi:10.1002/2014JA019919.

Thorne, R. M., W. Li, B. Ni, Q. Ma, J. Bortnik, L. Chen, D. N. Baker, H. E. Spence, G. D. Reeves, M. G. Henderson, C. A. Kletzing, W. S. Kurth, G. B. Hospodarsky, J. B. Blake, J. F. Fennell, S. G. Claudepierre, and S. G. Kanekal (2013), Rapid local acceleration of relativistic radiation-belt electrons by magnetospheric chorus, Nature, 504, 411, doi:10.1038/nature12889.

Tu, W., G. S. Cunningham, Y. Chen, S. K. Morley, G. D. Reeves, J. B. Blake, D. N. Baker, and H. Spence (2014), Event-specific chorus wave and electron seed population models in DREAM3D using the Van Allen Probes, Geophys. Res. Lett., 41, 1359–1366, doi:10.1002/2013GL058819.

Turner, D. L., V. Angelopoulos, W. Li, J. Bortnik, B. Ni, Q.Ma, R. M. Thorne, S. K. Morley, M. G. Henderson, G. D. Reeves, M. Usanova, I. R. Mann, S. G. Claudepierre, J. B. Blake, D. N. Baker, C.-L. Huang, H. Spence, W. Kurth, C. Kletzing, and J. V. Rodriguez (2014), Competing source and loss mechanisms due to wave-particle interactions in Earth's outer radiation belt during the 30 September to 3 October 2012 geomagnetic storm, J. Geophys. Res. Space Physics, 119, 1960–1979,10.1002/2014JA019770.

Ukhorskiy, A. Y., M. I. Sitnov, A. S. Sharma, B. J. Anderson, S. Ohtani, and A. T. Y. Lui (2004), Data-derived forecasting model for relativistic electron intensity at geosynchronous orbit, Geophys. Res. Lett., 31, L09806, doi:10.1029/2004GL019616.

Walker, A. D. M., (1971), The Propagation of Very Low-Frequency Radio Waves in Ducts in the Magnetosphere, Proceedings of the Royal Society of London. Series A, Mathematical and Physical Sciences, 321(1544), 69-93.

Weigel, R. S., A. J. Klimas, and D. Vassiliadis (2003), Precursor analysis and prediction of large-amplitude relativistic electron fluxes, Space Weather, 1(3), 1014, doi:10.1029/2003SW000023.

Xiao, F., C. Yang, Z. He, Z. Su, Q. Zhou, Y. He, C. A. Kletzing, W. S. Kurth, G. B. Hospodarsky, H. E. Spence, G. D. Reeves, H. O. Funsten, J. B. Blake, D. N. Baker, and J. R.Wygant (2014), Chorus acceleration of radiation belt relativistic electrons during March 2013 geomagnetic storm, J. Geophys. Res., 119, 3325–3332, doi:10.1002/2014JA019822.

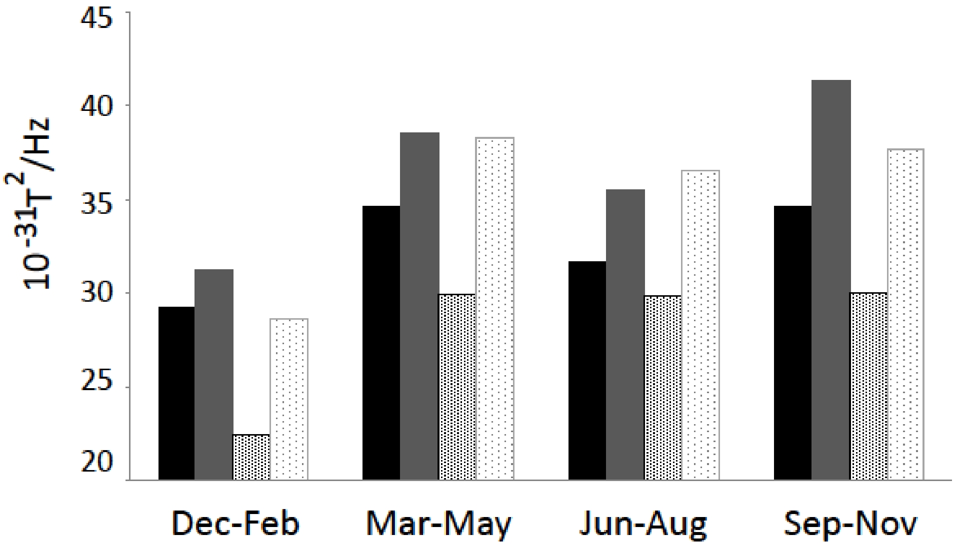

Figure 1. Ground VLF power following storms averaged by season. Black bars: VLF averaged over 0-48 hours following minimum Dst. Gray bars: VLF averaged over late recovery (48-72 hours following minimum Dst). Solid bars: VLF averaged over all hours of the day. Patterned: VLF averaged over the dawn period (9-12 UT).

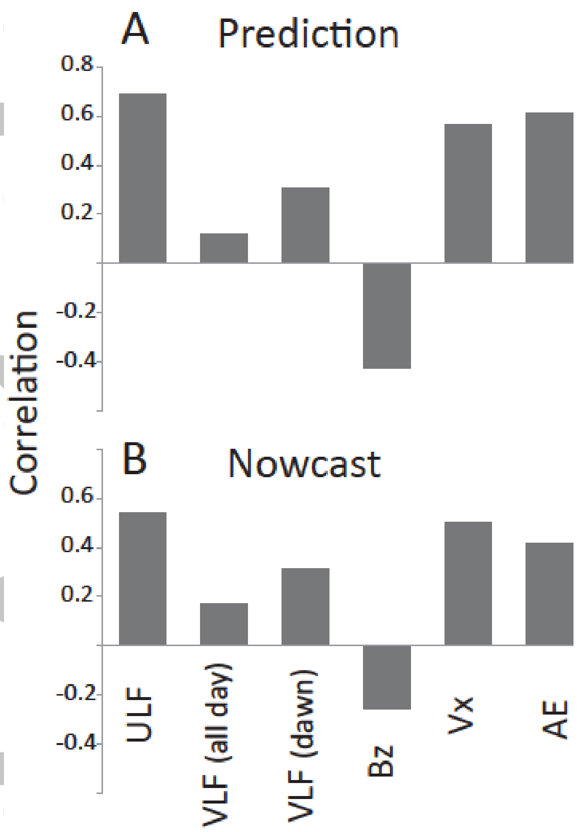

Figure 2. Correlations of variables with relativistic electron flux. All variables are averages from after the minimum Dst. A. Predictor variables (0-48 hours after minimum Dst), B. Nowcast variables (48-72 hours after minimum Dst). "All day" VLF averaged over all 24 hours of the day; "Dawn" VLF averaged over 9-12 UT.

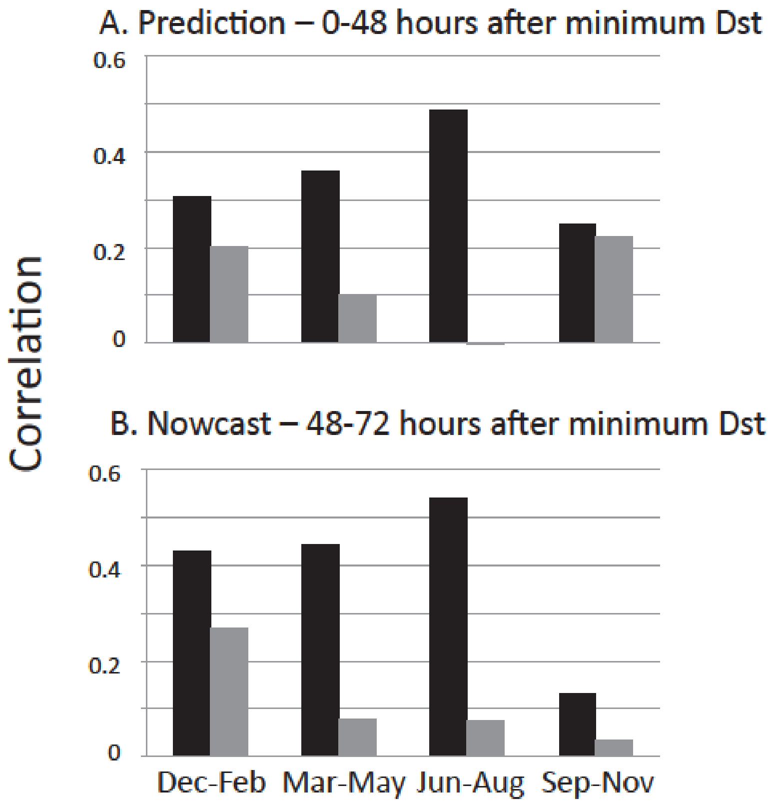

Figure 3. VLF-flux correlations by season and IMF Bz orientation. A. Prediction model (predictors measured 0-48 hours after minimum Dst), B. Nowcast (predictors measured 48-72 hours after minimum Dst). Black bars: northward IMF Bz, gray bars: southward IMF Bz. IMF Bz orientation is northward if average Bz 0-48 hours after minimum Dst was positive, southward if average Bz was negative. Correlation of 0.002 of VLF with relativistic electron flux during Jun-Aug southward Bz is too small to appear on this graph.

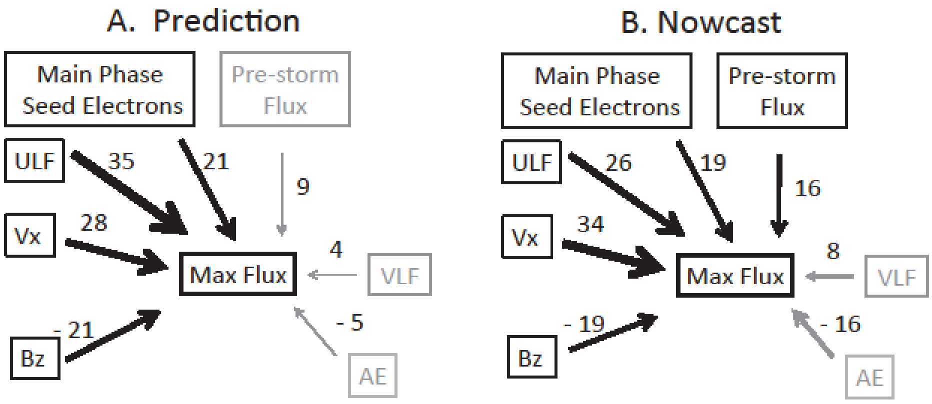

Figure 4. Influence of parameters over all seasons in A. the prediction model and B. the nowcast model. Numbers are standardized regression coefficients X 100. Black arrows represent significant parameters ($p<0.05$); grey arrows represent non-significant variables.

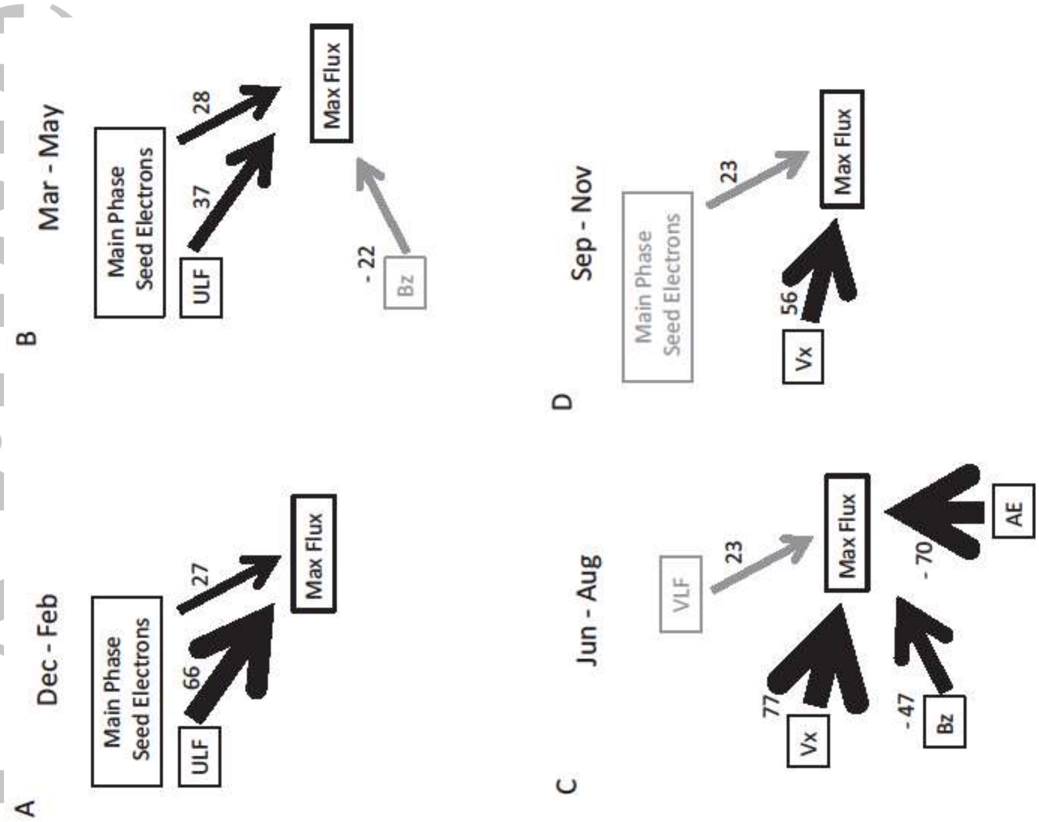

Figure 5. Nowcast model: influence of parameters by season (reduced models). Explanatory variables averaged over 48-72 hours following minimum Dst. A. Dec-Feb (n = 44), B. Mar-May (n = 60), C. Jun-Aug (n = 41), D. Sep-Nov (n = 46). Numbers are standardized regression coefficients X 100. Black arrows represent significant parameters ($p < 0.05$); grey arrows represent non-significant variables.

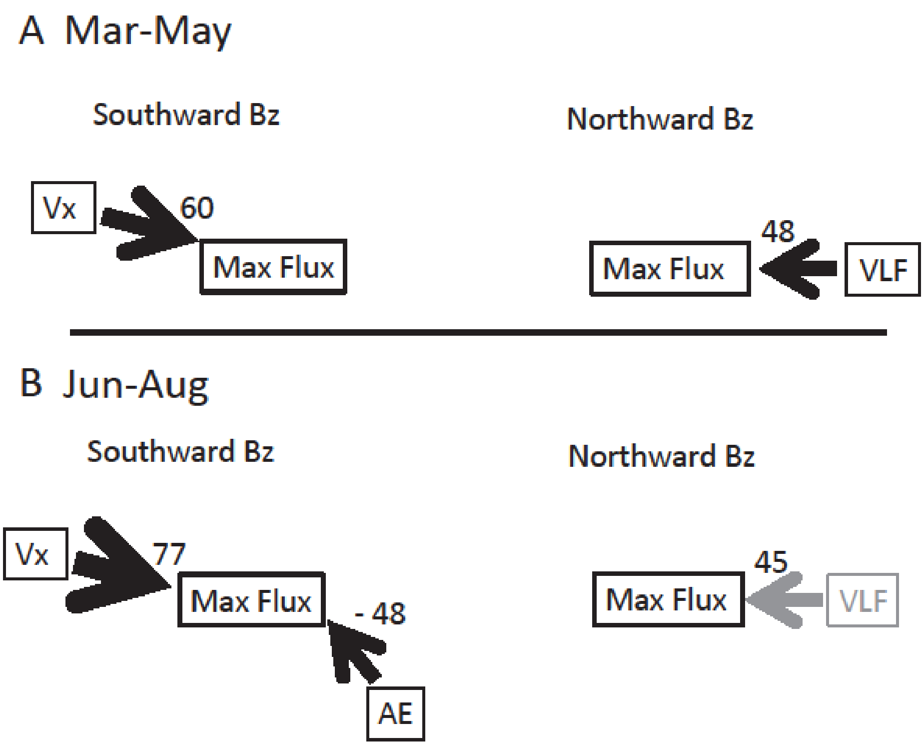

Figure 6. Reduced nowcast models for southern hemisphere winter months, broken down by IMF Bz orientation. A. Mar-May (southward n = 32, northward n = 28) B. Jun-Aug (southward n = 24, northward n = 17). IMF Bz orientation is northward if Bz averaged over the 48-72 hrs following minimum Dst was positive, southward if average Bz was negative.

.

Table 1. Correlation of VLF wave power (9-12 UT) with relativistic electron flux (rankit transformations). L_{max} from Smith et al. [2004]. N=190 storms.

VLF Channel	Prediction[a]	Nowcast[b]	L_{max}
.5 kHz	0.238*	0.254*	9.47
1.0 kHz	0.308*	0.316*	7.52
2.0 kHz	0.054	0.038	5.96
4.25 kHz	-0.043	-0.025	4.64

a: VLF measured 0-48 hrs after min Dst
b: VLF measured 48-72 hrs after min Dst
*: significant correlation ($p < 0.05$)